Am J Transl Res 2018;10(2):444-454
www.ajtr.org /ISSN:1943-8141/AJTR0065477

Original Article

Multi-parameter evaluation of lumbar intervertebral disc degeneration using quantitative magnetic resonance imaging techniques

Xuanqi Xiong[1], Zhengwei Zhou[2], Matteo Figini[3], Junjie Shangguan[3], Zhuoli Zhang[3], Wei Chen[1]

[1]Department of Radiology, Southwest Hospital, Third Military Medical University (Army Medical University), Chongqing 400038, China; [2]Biomedical Imaging Research Institute, Cedars-Sinai Medical Center, Los Angeles, CA, USA; [3]Department of Radiology, Feinberg School of Medicine-Northwestern University, Chicago, IL 60611, USA

Received September 12, 2017; Accepted January 10, 2018; Epub February 15, 2018; Published February 28, 2018

Abstract: *Objective:* To quantitatively evaluate lumbar disc degeneration with recently-developed quantitative magnetic resonance imaging (MRI) techniques. A series of MRI parameters, including T2*, T1rho relaxation time, apparent diffusion coefficient and gagCEST, were compared and correlated with the Pfirrmann semi-quantitative classification of lumbar intervertebral disc degeneration; the most accurate and relevant MRI parameters of lumbar disc degeneration were identified. *Materials and Methods:* Thirty-seven subjects (age range, 18-74 years) with non-specific low back pain (LBP) for more than 6 months were enrolled. The L1/2-L5/S1 discs of each subject were measured and then analyzed. *Results:* The gagCEST value of the discs showed the best negative correlation with degeneration level (nucleus pulposus: r = -0.951, $P < 0.001$; annulus fibrosus: r = -0.938, $P < 0.001$). The discriminant analysis results showed that this parameter also had the highest correct rate using a single index (gagCEST discriminant accuracy = 82%). *Conclusion:* Early stage lumbar disc degeneration can be quantitatively evaluated with MRI using the chemical exchange saturation transfer technique.

Keywords: Lumbar disc degeneration, chemical exchange saturation transfer, gagCEST

Introduction

Modern evidence-based medicine has identified intervertebral disc degeneration (IVDD) as a consequence of a variety of genetic, traumatic, mental, and nutritional factors. Recent studies have reported that IVDD, which can start as early as childhood [1], has become a serious social burden due to the enormous associated medical costs [2]. Although the reasons for low back pain (LBP) in most cases are not completely clear and, at present, only 15% of cases are accurately diagnosed and treated [3], the lumbar intervertebral discs are typically considered as the most common pathogenesis of LBP. With aging, the degree of IVDD and the incidence of LBP mutually increase, suggesting that IVDD may be the primary cause of LBP [4]. However, the early signs of IVDD include imperceptible changes in biochemical metabolism within discs, such as the loss of water and glycosaminoglycan (GAG), as well as decreased osmotic pressure and pH, which cannot be easily detected by conventional imaging and clinical examinations. IVDD is usually first detected upon the manifestation of some morphological abnormality observed by imaging, but clinical interventional options at that stage are limited to conservative treatment alone or surgical excision. Therefore, early and quantitative diagnosis of IVDD is very important to reestablish and regenerate degenerated lumbar intervertebral discs. Pfirrmann, a Swiss orthopedist, and his colleagues proposed semi-quantitatively dividing IVDD into five grades according to morphological changes, magnetic resonance (MR) signal intensity, and the discrimination of the nucleus pulposus (NP) and annulus fibrosus (AF) of the discs [5, 6]. Even though the Pfirrmann grade is widely applied in clinical practice worldwide, this classification system is very subjective and ambiguous due to the lack of a quantitative index, thereby restricting the ability to detect IVDD at an early stage.

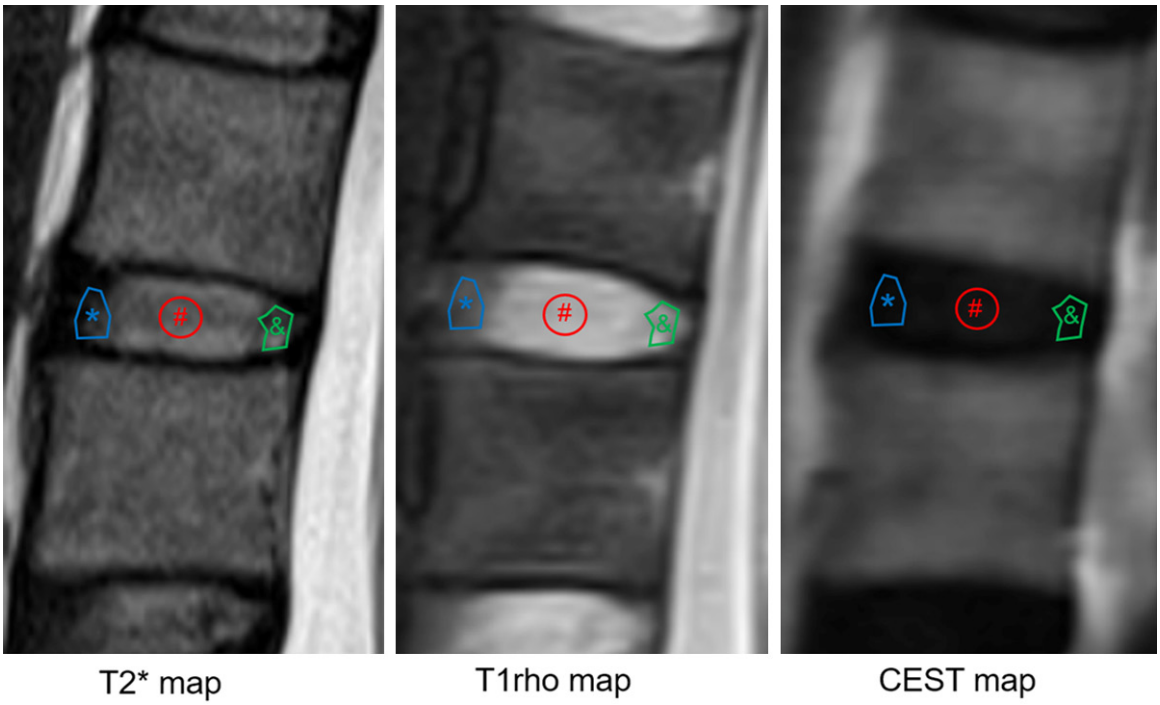

Figure 1. A schematic diagram of the ROIs. Examples of ROIs over NP (#), anterior AF (*) and posterior AF (&) in one disc are shown.

Table 1. T2* relaxation time and ADC value of the 185 lumbar discs according to the Pfirrmann grade

Pfirrmann grades	n (%)#		T2* (ms)		ADC (mm^2/s)	
			NP	AF	NP	AF
I	42 (22.7)	Median	53.4	44.6	1.47	1.24
		Mean	57.8	45.0	1.48	1.25
		SD	19.3	13.9	0.15	0.17
II	50 (27)	Median	44.8	30.9	1.27	1.01
		Mean	47.4	32.1	1.25	0.98
		SD	14.8	10.1	0.14	0.18
III	28 (15.1)	Median	38.5	31.2	0.99	0.86
		Mean	39.6	30.5	0.99	0.84
		SD	9.8	6.6	0.18	0.14
IV	34 (18.4)	Median	30.7	25.0	0.79	0.71
		Mean	30.3	25.4	0.79	0.73
		SD	5.2	4.9	0.14	0.14
V	31 (16.8)	Median	24.2	21.4	0.55	0.56
		Mean	22.5	20.1	0.53	0.55
		SD	7.7	6.3	0.14	0.12

NP, nucleus pulposus; AF, annulus fibrosus; #, percentage of each group of sample content overall.

With the rapid development of quantitative MR imaging (MRI), many noninvasive and non-radioactive imaging diagnostic methods have already been used to quantitatively explore the process of IVDD, which include *in vivo* Na MRI, quantitative high-resolution magic angle spinning nuclear MR (NMR) spectroscopy, proton T2 imaging, T1rho imaging and diffusion tensor imaging [7-11]. A series of quantitative MR parameters, including the T1rho relaxation time (T1rho), apparent diffusion coefficient (ADC), and fractional anisotropy (FA), are useful to detect some imperceptible biochemical changes within the discs that otherwise would be overlooked with conventional MRI. However the intrinsic associations between these quantitative MR parameters and the biological properties of the disc tissues have not yet been completely elucidated.

Chemical exchange saturation transfer (CEST), a recent novel MRI technique, can monitor changes in MR signals produced by alterations of certain biochemical molecules in tissues, such as proteins, amino acids, and GAG, as well as pH. CEST has already been widely used in a number of areas of quantitative medical research, especially in the fields of oncology and neurology [12-16]. Previous studies have confirmed that IVDD is closely related to

Table 2. T1rho relaxation time of the 132 lumbar discs according to the Pfirrmann grade

Pfirrmann grades	n' (%)		T1rho (ms)	
			NP	AF
I	25 (18.9)	Median	143.11	109.59
		Mean	150.23	100.72
		SD	50.61	31.75
II	38 (28.8)	Median	95.23	69.78
		Mean	99.22	68.56
		SD	20.45	14.12
III	20 (15.2)	Median	69.25	59.57
		Mean	70.08	59.90
		SD	6.15	9.59
IV	25 (18.9)	Median	52.09	46.66
		Mean	54.67	49.36
		SD	10.32	12.95
V	24 (18.2)	Median	41.75	37.40
		Mean	42.64	37.30
		SD	6.29	5.47

NP, nucleus pulposus; AF, annulus fibrosus.

Table 3. gagCEST values of the 117 lumbar discs according to the Pfirrmann grade

Pfirrmann grades	n" (%)		gagCEST	
			NP	AF
I	31 (26.5)	Median	580.16	560.87
		Mean	589.23	566.96
		SD	29.24	27.54
II	27 (23.1)	Median	543.81	533.00
		Mean	545.48	537.20
		SD	13.27	15.64
III	19 (16.2)	Median	509.56	512.06
		Mean	502.51	507.95
		SD	19.51	21.89
IV	24 (20.5)	Median	474.18	479.27
		Mean	475.67	474.96
		SD	26.41	22.20
V	16 (13.8)	Median	363.16	367.26
		Mean	354.15	365.84
		SD	49.76	51.53

NP, nucleus pulposus; AF, annulus fibrosus.

the loss of GAG within discs [17, 18]. Consequently GAG CEST (gagCEST) MRI has been applied to quantitative MRI of the discs, mainly to monitor the GAG content of discs. A phantom study reported a significant positive correlation between the gagCEST value, the major parameter in gagCEST MRI, and the actual GAG concentration [19]. Another small-scale human study demonstrated that the gagCEST value of the discs was negatively correlated with the Pfirrmann grade as well as the T2 value [20]. Therefore, the aim of the present study was to quantitatively evaluate the usefulness of gagCEST MRI for the early diagnosis of IVDD and to combine this with other MR parameters (i.e., the T2*, ADC, and T1rho value) for comparative analysis. In addition, Pfirrmann grades were correlated with the most sensitive and relevant MR parameter for early and quantitative imaging diagnosis of IVDD.

Materials and methods

Subjects

The cohort of this prospective study comprised a total of 37 subjects (16 males and 21 females; mean age, 48.3 years; range: 18-74 years) who met the inclusion criteria of non-specific LBP for more than 6 months and age ≥ 18 years. The exclusion criteria included lumbar trauma, previous lumbar surgery, infection, tuberculosis, tumor, or other severe lumbar diseases, ankylosing spondylitis, metal internal fixation implants or implantation of a metal stent pacemaker, and claustrophobia. Five lumbar discs (L1/2-L5/S1) were tested in each subject. A total of 185 discs were divided into five groups according to the five-level Pfirrmann grading system [5, 6] by two primary radiologists (with 3 and 5 years of experience, respectively). In case of differing opinions, consensus was reached by discussion with a senior radiologist with 20 years of osteoarticular working experience. Sagittal T2* mapping, CEST, diffusion, and T1rho-weighted images of these 185 discs were collected and regions of interest (ROIs) were delineated and used to measure all the quantitative parameters.

MRI protocol

All images were captured using a Siemens MAGNETOM Trio 3.0T MRI system (Siemens Healthineers, Erlangen, Germany). The imaging protocol included sagittal conventional T2-weighted imaging, diffusion-weighted imaging (DWI), T1rho, and gagCEST sequences. First, conventional sagittal T2-weighted images were obtained using a turbo spin echo sequence

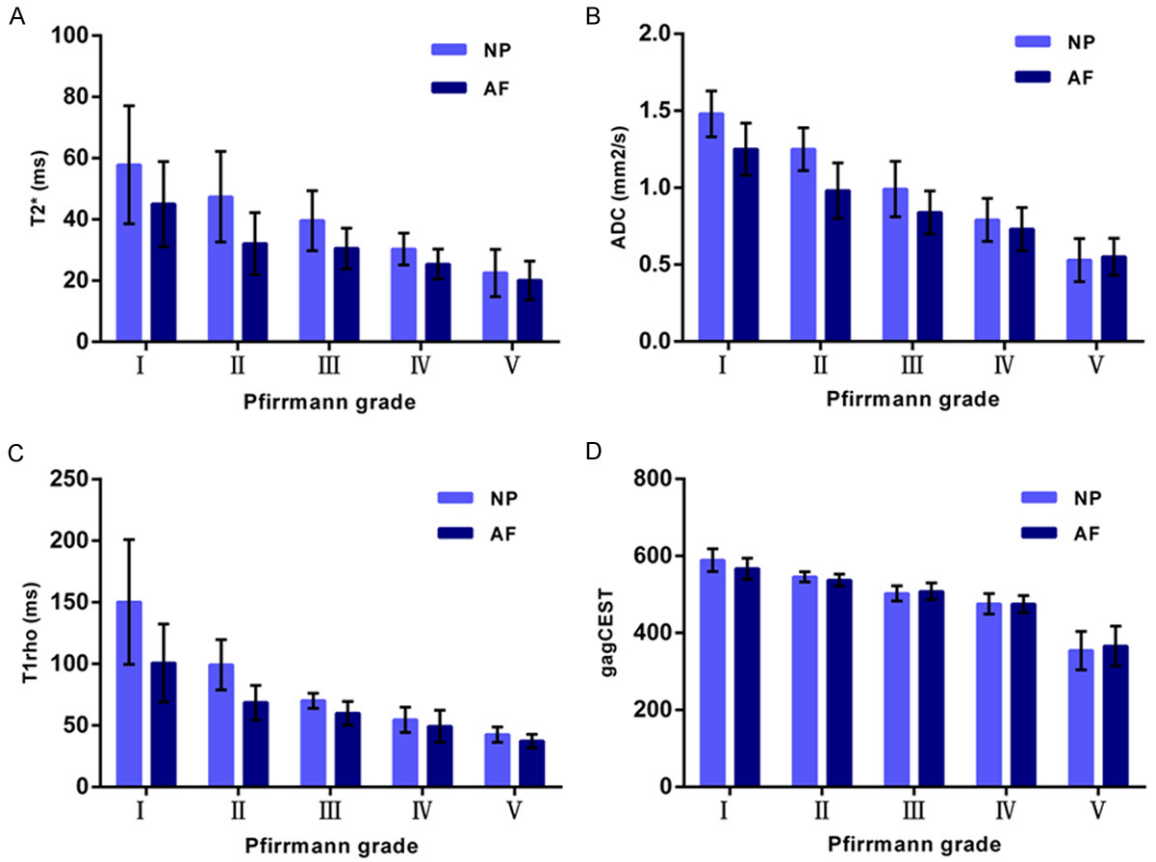

Figure 2. The distribution of the values of NP and AF with respect to the Pfirrmann grade. A: T2* relaxation time of NP and AF versus disc degeneration grading; B: ADC value of NP and AF versus disc degeneration grading; C: T1rho relaxation time of NP and AF versus disc degeneration grading; D: GagCEST value of NP and AF versus disc degeneration grading.

with the following parameters: repetition time (TR)/echo time (TE) = 3200 ms/89 ms, number of slices (NSL) = 13, slice thickness = 3 mm, and field of view (FOV) = 329 × 329 mm^2. Next, a series of sagittal T2*, DWI, T1rho and CEST quantification sequences were obtained. The T2* images were acquired with: TR/TE = 90 ms/3.29, 8.66, 14.03, 19.4, 24.77, 30.14, 35.51, and 40.88 ms, NSL = 6, slice thickness = 3 mm, and FOV = 350 × 350 mm^2. The DWI sequences were obtained with: TR/TE = 2000 ms/77 ms, NSL = 11, slice thickness = 2 mm, FOV = 300 × 400 mm^2, diffusion gradient factor (b value) = 0, 250, 500, 1000, and 1500 s/mm^2, diffusion directions = 3, bandwidth = 1750 Hz/Px. The T1rho-weighted images were obtained using a single slice (the middle slice of the T2-weighted images) sequence with: TR/TE = 4000 ms/8.9 ms, FOV = 220 × 220 mm^2, and bandwidth = 1750 Hz/Px. The CEST sequences included two sequences (the CEST sequence and the water saturation shift referencing [WASSR] sequence) with: a single slice (the same slice with T1rho sequence), FOV = 68 × 220 mm^2, bandwidth = 299 Hz/Px, and TR/TE = 3500 ms/9.1 ms (WASSR sequence) and 9000 ms/8.8 ms (CEST sequence).

Image post-processing

T1rho maps were generated by pixel-by-pixel fitting to the following equation: S (TSL) = S0 *exp (-TSL/T1rho), where TSL is the spin-locking time, S is the signal intensity of the T1rho-weighted images, and S0 is the signal intensity when TSL = 0. GagCEST maps were reconstructed with the following equation: MTRasym = Z (-Δω) - Z (+Δω), where Δω is the resonant frequency of GAG protons (1.0 ppm). The B0 field was corrected using the WASSR method [21].

ROI measurement

Three ROIs with an area of 25-30 mm^2 were designated for every disc on the selected imag-

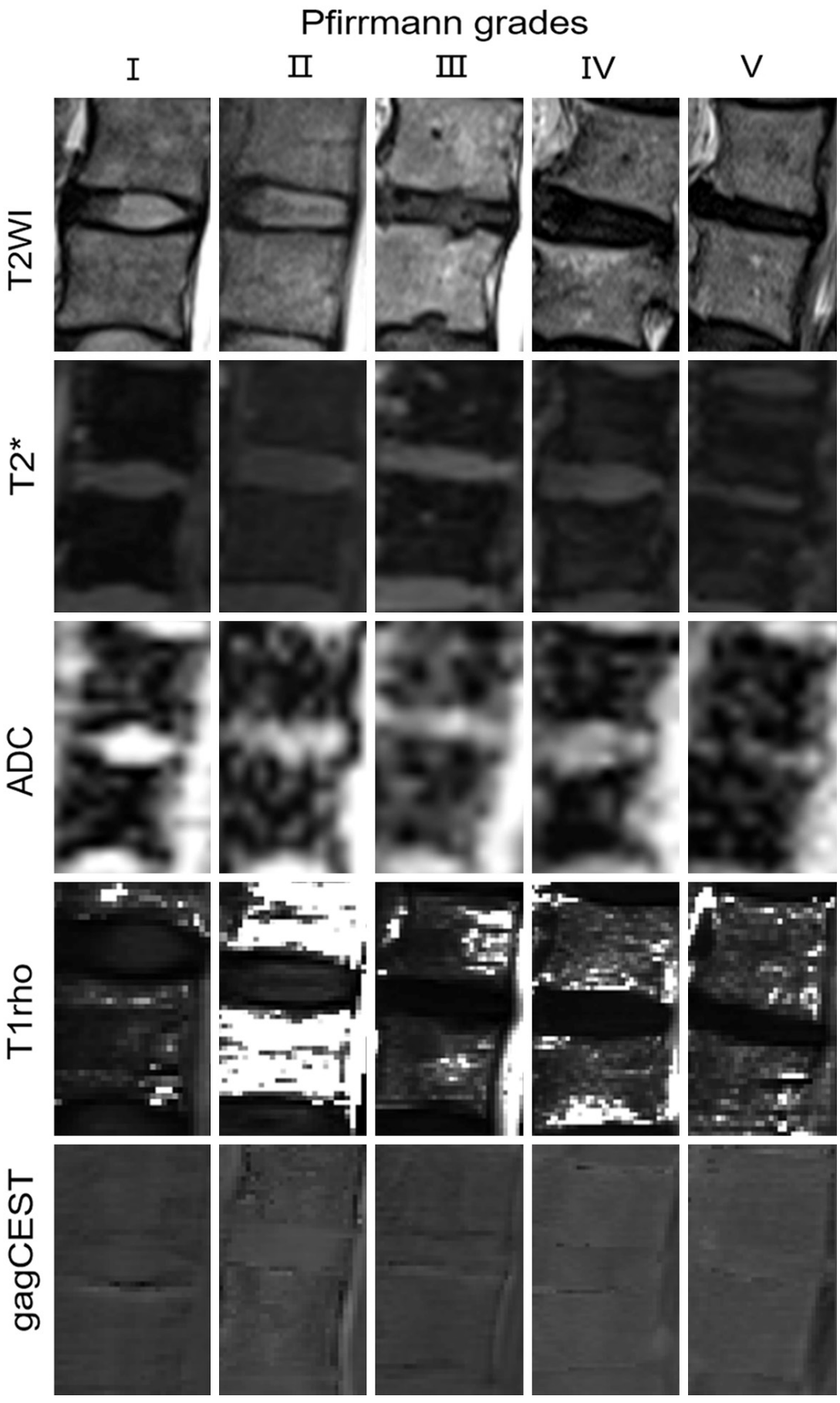
Pfirrmann grades
I
II
III
IV
V
T2WI
T2*
ADC
T1rho
gagCEST

Figure 3. T2-weighted sagittal images and corresponding T2*, ADC, T1rho and gagCEST maps in representative lumbar disc degeneration related to Pfirrmann grades.

Table 4. ICCs with 95% CIs for each parameter at different ROIs

MR parameters	ROIs	ICC	95% CI
T2* relaxation time (ms)	NP	0.769	0.701-0.832
	AAF	0.789	0.733-0.851
	PAF	0.752	0.715-0.828
ADC value (mm^2/s)	NP	0.904	0.868-0.937
	AAF	0.895	0.857-0.912
	PAF	0.890	0.849-0.910
T1rho relaxation time (ms)	NP	0.935	0.879-0.958
	AAF	0.925	0.871-0.949
	PAF	0.931	0.869-0.951
gagCEST value	NP	0.951	0.923-0.969
	AAF	0.948	0.918-0.958
	PAF	0.939	0.908-0.947

ROI, regions of interest; NP, nucleus pulposus; AAF, anterior annulus fibrosus; PAF, posterior annulus fibrosus.

es, which represented the NP, anterior AF (AAF), and posterior AF (PAF), respectively. The mean AAF and PAF values represented the value of the whole AF. The anteroposterior positions approximately corresponded to the anterior, middle, and posterior column of the vertebral body (**Figure 1**). The ROIs were either inferior or superior to the endplate of the vertebral body. The T2*, T1rho, ADC, and gagCEST values were measured using Image J software (https://imagej.nih.gov/ij/). Using the same method, all ROIs were mapped on the same image 3 months later in order to remeasure the MR parameters and calculate the intraclass correlation coefficient (ICC).

Statistical analysis

All statistical analyses were performed using SPSS version 22.0 software (IBM Corp., IBM Corp., Armonk, NY, USA). The five Pfirrmann grades were compared by one-way analysis of variance if the variance was homogeneous or the Kruskal-Wallis H test if the variance was not homogeneous. Post hoc multiple comparisons were performed using Tamhane's T2 test. Correlations were identified with the Spearman rank correlation coefficient. Fisher linear discriminant analysis was performed by the single-index stepwise discriminant method. The ICC and 95% confidence intervals (95% CIs) were calculated to assess the reproducibility of the two measurements. ICC ≥ 0.75 was considered an excellent agreement [22].

Results

Pfirrmann grading

The sagittal T2-weighted images of the 185 discs (L1/2-L5/S1 of 37 subjects) were divided into five groups according to the five-level Pfirrmann grading [5, 6], as follows: grade I (normal group): n1 = 42 (22.7%); grade II (mild degeneration group): n2 = 50 (27%); grade III (moderate degeneration group): n3 = 28 (15.1%); grade IV (severe degeneration group): n4 = 34 (18.4%); and grade V (extremely severe degeneration group): n5 = 31 (16.8%) (**Table 1**). Of the T1rho sequences, images of 53 discs were excluded because of the presence of motion artifacts, so the actual effective sample content of the T1rho weighted images was n' = 132 discs: grade I: n1' = 25 (18.9%); grade II: n2' = 38 (28.8%); grade III: n3' = 20 (15.2%); grade IV: n4' = 25 (18.9%); and grade V: n5' = 24 (18.2%) (**Table 2**). The CEST sequences of 68 images were also excluded due to the presence of motion artifacts, so the actual effective sample content of the CEST images was n" = 117 discs: grade I: n1" = 31 (26.5%); grade II: n2" = 27 (23.1%); grade III: n3" = 19 (16.2%); grade IV: n4" = 24 (20.5%); and grade V: n5" = 16 (13.8%) (**Table 3**).

Evaluation of NP and AF

The statistical results of T2* relaxation time (T2*: ms), ADC value (ADC: mm^2/s), T1rho relaxation time (T1rho: ms), and gagCEST value (gagCEST: no unit) of the NP and AF (the mean value of the AAF and PAF) from the ROIs are presented in **Tables 1-3** and **Figure 2**. Representative T2-weighted sagittal images related to Pfirrmann grades and the corresponding T2*, ADC, T1rho, and gagCEST maps of the lumbar discs are shown in **Figure 3**.

To reflect the reliability of the two measurements, ICCs with 95% CIs for each parameter at different ROIs are shown in **Table 4**. The values demonstrated that the reproducibility

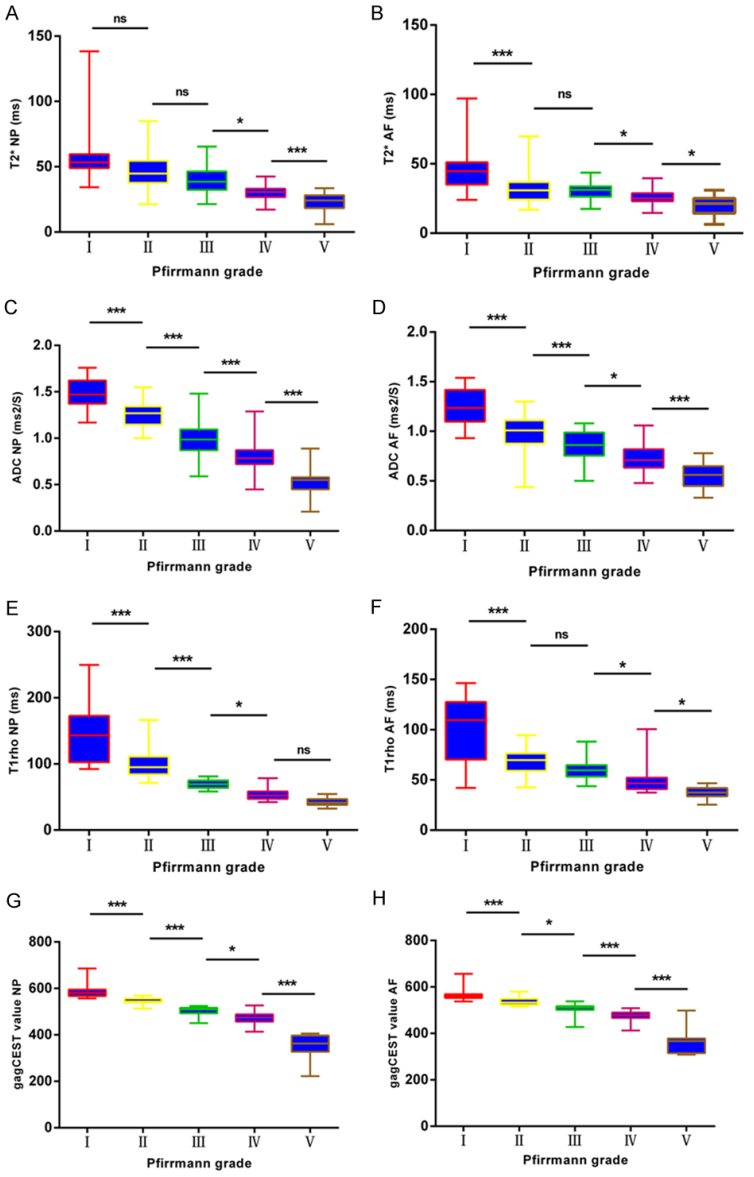

Figure 4. Box plots of the values versus disc degeneration grading. The results of post-hoc multiple comparisons between two groups of adjacent discs are shown. Trends of decreasing T2*, T1rho, ADC and gagCEST values of nucleus pulposus (NP) and annulus fibrosus (AF) with increasing Pfirrmann grades can also be seen. (A) and (B) are respectively T2* relaxation time of NP and AF versus disc degeneration grading; (C) and (D) are respectively ADC value of NP and AF versus disc degeneration grading; (E) and (F) are respectively T1rho relaxation time of NP and AF versus disc degeneration grading; (G) and (H) are respectively gagCEST value of NP and AF versus disc degeneration grading. *P < 0.05; ***P < 0.001; "ns" = not significant.

between the two measurements was excellent (ICC ≥ 0.75).

Boxplots of T2*, ADC, T1rho, and gagCEST values of the lumbar discs according to the Pfirrmann grade are shown in **Figure 4**. Comparisons between multiple groups by one-way analysis of variance or the Kruskal-Wallis H test all showed highly significant differences in T2*, ADC, T1rho, and gagCEST values of NP and AF among the Pfirrmann grade groups (P < 0.001). The results of post-hoc multiple comparisons (only one step between the two comparisons with no comparison across levels) of NP using Tamhane's T2 test showed that all between-group differences were significant, with the exception of T2* between Pfirrmann grades I and II, and grades II and III, as well as the T1rho relaxation time between Pfirrmann grades IV and V. The results of post-hoc multiple comparisons of AF showed that all between-group differences were significant, with the exception of T2* between Pfirrmann grades II and III and the T1rho relaxation time between Pfirrmann grades II and III.

Furthermore, the results also showed higher significant differences in gagCEST values between Pfirrmann grades I and II for NP than the T2* relaxation time, which revealed that gagCEST was capable of detecting early IVDD.

Correlation analysis

Spearman rank correlation analysis results demonstrated that the T2*, ADC, T1rho, and gagCEST values were inversely significantly correlated with the Pfirrmann grades for both NP and AF (**Figure 5**). The correlation coefficients were as follows: T2* (NP: r = -0.783, P < 0.001; AF: r = -0.683, P < 0.001), ADC value (NP: r = -0.914, P < 0.001; AF: r = -0.843, P < 0.001), T1rho relaxation time (NP: r = -0.926, P < 0.001; AF: r = -0.803, P < 0.001), and gagCEST value (NP: r = -0.951, P < 0.001; AF: r = -0.938, P < 0.001).

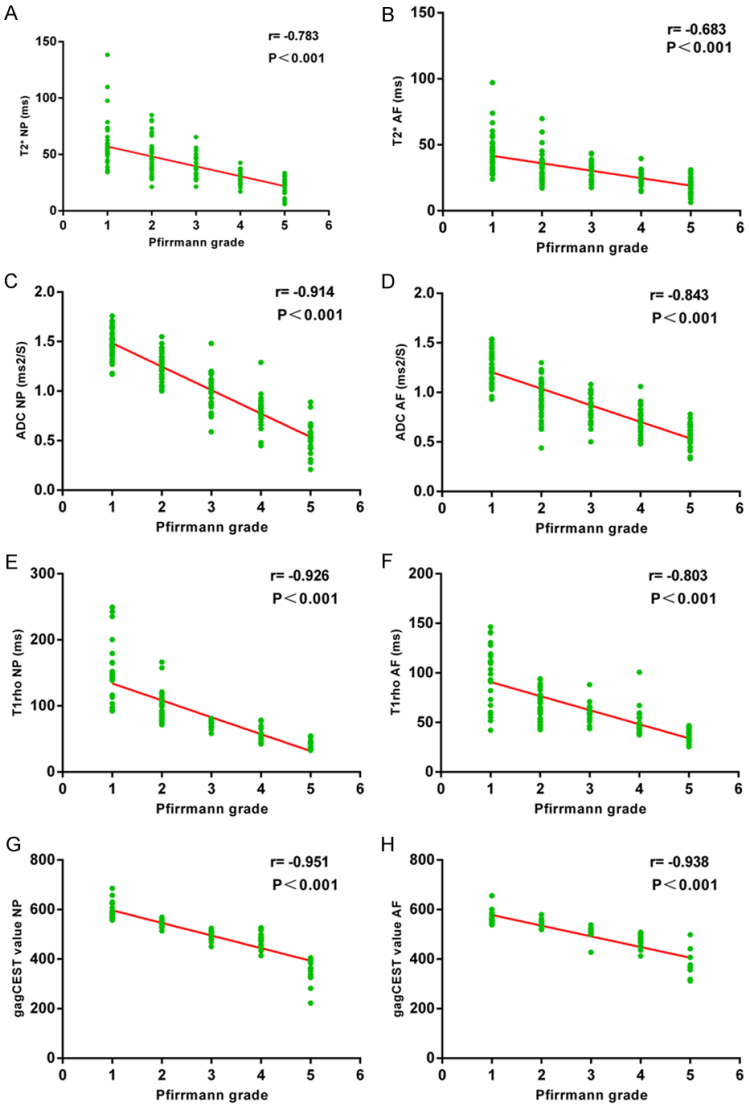

Figure 5. Scatter plots of the values in nucleus pulposus (NP) and annulus fibrosus (AF) according to the Pfirrmann grades. (A) and (B) are respectively T2* relaxation time of NP and AF correlated with disc degeneration grading; (C) and (D) are respectively ADC value of NP and AF correlated with disc degeneration grading; (E) and (F) are respectively T1rho relaxation time of NP and AF correlated with disc degeneration grading; (G) and (H) are respectively gagCEST value of NP and AF correlated with disc degeneration grading.

The results also showed the gagCEST value had a higher correlation with the Pfirrmann grades than the other MR parameters both for NP and AF.

Discriminant analysis

Interference of the artifacts was excluded by filtering the NP values of 89 of the 185 discs, which all contained the four parameters of T2*, ADC, T1rho, and gagCEST. Then, the values were subjected to Fisher's linear discriminant analysis. The results of the Pfirrmann grades and the single-index discriminant of the NP values of these 89 discs are shown in **Table 5**, and the discriminant accuracy is shown in **Table 6** (accuracy was the ratio of the correct discriminant discs to the 89 discs). The results revealed the gagCEST parameter had a higher discriminatory rate than the other indices.

Discussion

In this study, a novel quantitative MRI technique was used to noninvasively explore the biochemical metabolic abnormalities within degenerated lumbar discs, such as the loss of GAG and disordered diffusion of water molecules. As compared with the semi-quantitative Pfirrmann grades assigned to conventional sagittal T2-weighted images of lumbar discs, the T2*, ADC, T1-rho, and gagCEST values all showed negative correlations and highly significant differences between groups, especially in the gagCEST value. The T2* value is closely related to the water content in biological tissue, but the results of this study indicated that there was no significant difference in the T2* relaxation time between Pfirrmann grades I (normal group) and II (mild degeneration group) for NP, confirming that there was only a reduction in GAG content, but no or little water loss or morphological changes within the early degenerated discs [23, 24]. This demonstrates that the ability to diagnose early stage IVDD by conventional T2-weighted images or T2*-mapping is very limited. However, T1rho and CEST MRI can make up for this short-coming [25, 26].

Previous studies have confirmed that the earlier that IVDD is detected and diagnosed, the more beneficial any clinical treatment or reconstruction and regeneration of the lumbar disc

Table 5. Pfirrmann grades and discriminant analysis of the NP of the 89 discs

Pfirrmann grades		T2*	ADC	T1rho	gagCEST
I	19	14	21	14	20
II	22	22	21	20	22
III	16	16	11	26	15
IV	18	24	22	13	17
V	14	13	14	16	15
Total	89	89	89	89	89

Table 6. Discriminant accuracy of the four parameters

Parameters	Discriminant accuracy
T2*	47.2%
ADC	69.7%
T1rho	71.9%
gagCEST	82.0%

will be [27, 28]. However, the current semi-quantitative Pfirrmann grades provide neither quantitative nor objective assessment criteria for the diagnosis of IVDD. The gagCEST value in this study had the highest correlation with Pfirrmann grades and provided the greatest discrimination among the considered MR parameters. In addition, the greater significant difference between Pfirrmann grades I and II of NP than T2* relaxation time revealed that in the near future, early and quantitative evaluation of IVDD can be achieved with the use of the quantitative CEST MRI method to noninvasively assess the GAG content within the disc. However, at present, CEST MRI is rarely applied in clinical practice, in comparison to conventional T2-weighted imaging or DWI, for various reasons such as the long scan time (a single-slice CEST sequence may require 40-50 min), the stringent requirements for magnetic field intensity and shimming, and the lack of image post-processing software.

Although the results of this prospective clinical diagnostic study showed certain superiority in the diagnosis of IVDD, there were some limitations that should be addressed. First, the lack of experience with the T1rho and CEST sequences required more time than expected and various images had to be excluded due to motion artifacts, which led to an insufficient sample size. Second, disc tissue specimens could not be acquired by surgery or puncture because of the restrictions of medical ethics and other factors. Therefore, the five-level Pfirrmann grade was adopted as a relative gold standard for IVDD instead of histological analysis. Third, we were unable to combine a series of related clinical symptoms of IVDD, such as LBP, to more deeply explore the association with the degree of degeneration in the images, partly because clinical symptoms such as LBP are influenced by many factors and are not necessarily consistent with the imaging findings [29]. Finally, in the experimental process, the discs of subjects with lumbar disc herniation were deviated from the normal anatomical positions. In such a case, the monitored MR parameters will not be in agreement with the designating method of the ROI in this study. Consequently, we suggest that future similar studies should include only IVDD subjects without disc herniation.

Conclusion

In the process of lumbar disc degeneration, the loss of GAG content within the NP and AF can be quantified by the CEST MRI technique, even in the early stage. Furthermore, the gagCEST value of NP and AF revealed an excellent negative correlation with the five-level Pfirrmann degeneration grades, higher than the other MR parameters in this study. Therefore, the CEST MRI method should be considered for early diagnosis and quantitative evaluation of IVDD.

Disclosure of conflict of interest

None.

Address correspondence to: Dr. Wei Chen, Department of Radiology, Southwest Hospital, Third Military Medical University (Army Medical University), Chongqing 400038, China. Tel: +8613508383249; Fax: +862365463026; E-mail: landcw@hotmail.com

References

[1] Adams MA and Roughley PJ. What is intervertebral disc degeneration, and what causes it? Spine (Phila Pa 1976) 2006; 31: 2151-2161.
[2] Maniadakis N and Gray A. The economic burden of back pain in the UK. Pain 2000; 84: 95-103.
[3] Andersson GB. Epidemiology of low back pain. Acta Orthop Scand Suppl 1998; 281: 28-31.

[4] Deyo RA and Weinstein JN. Low back pain. N Engl J Med 2001; 344: 363-370.
[5] Pfirrmann CW, Metzdorf A, Zanetti M, Hodler J and Boos N. Magnetic resonance classification of lumbar intervertebral disc degeneration. Spine (Phila Pa 1976) 2001; 26: 1873-1878.
[6] Urrutia J, Besa P, Campos M, Cikutovic P, Cabezon M, Molina M and Cruz JP. The pfirrmann classification of lumbar intervertebral disc degeneration: an independent inter- and intra-observer agreement assessment. Eur Spine J 2016; 25: 2728-33.
[7] Insko EK, Clayton DB and Elliott MA. In vivo sodium MR imaging of the intervertebral disk at 4 T. Acad Radiol 2002; 9: 800-804.
[8] Keshari KR, Zektzer AS, Swanson MG, Majumdar S, Lotz JC and Kurhanewicz J. Characterization of intervertebral disc degeneration by high-resolution magic angle spinning (HR-MAS) spectroscopy. Magn Reson Med 2005; 53: 519-527.
[9] Antoniou J, Demers CN, Beaudoin G, Goswami T, Mwale F, Aebi M and Alini M. Apparent diffusion coefficient of intervertebral discs related to matrix composition and integrity. Magn Reson Imaging 2004; 22: 963-972.
[10] Wang YX, Zhao F, Griffith JF, Mok GS, Leung JC, Ahuja AT and Yuan J. T1rho and T2 relaxation times for lumbar disc degeneration: an in vivo comparative study at 3.0-Tesla MRI. Eur Radiol 2013; 23: 228-234.
[11] Wang YX, Griffith JF, Leung JC and Yuan J. Age related reduction of T1rho and T2 magnetic resonance relaxation times of lumbar intervertebral disc. Quant Imaging Med Surg 2014; 4: 259-264.
[12] Ling W, Regatte RR, Navon G and Jerschow A. Assessment of glycosaminoglycan concentration in vivo by chemical exchange-dependent saturation transfer (gagCEST). Proc Natl Acad Sci U S A 2008; 105: 2266-2270.
[13] Zhou J, Lal B, Wilson DA, Laterra J and van Zijl PC. Amide proton transfer (APT) contrast for imaging of brain tumors. Magn Reson Med 2003; 50: 1120-1126.
[14] Farrar CT, Buhrman JS, Liu G, Kleijn A, Lamfers ML, McMahon MT, Gilad AA and Fulci G. Establishing the Lysine-rich protein CEST reporter gene as a CEST MR imaging detector for oncolytic virotherapy. Radiology 2015; 275: 746-754.
[15] Deng M, Chen SZ, Yuan J, Chan Q, Zhou J and Wang YX. Chemical exchange saturation transfer (CEST) MR technique for liver imaging at 3.0 Tesla: an evaluation of different offset number and an after-meal and over-night-fast comparison. Mol Imaging Biol 2016; 18: 274-282.
[16] Jones CK, Polders D, Hua J, Zhu H, Hoogduin HJ, Zhou J, Luijten P and van Zijl PC. In vivo three-dimensional whole-brain pulsed steady-state chemical exchange saturation transfer at 7 T. Magn Reson Med 2012; 67: 1579-1589.
[17] Lipson SJ and Muir H. 1980 Volvo award in basic science. Proteoglycans in experimental intervertebral disc degeneration. Spine (Phila Pa 1976) 1981; 6: 194-210.
[18] Lyons G, Eisenstein SM and Sweet MB. Biochemical changes in intervertebral disc degeneration. Biochim Biophys Acta 1981; 673: 443-453.
[19] Kim M, Chan Q, Anthony MP, Cheung KM, Samartzis D and Khong PL. Assessment of glycosaminoglycan distribution in human lumbar intervertebral discs using chemical exchange saturation transfer at 3 T: feasibility and initial experience. NMR Biomed 2011; 24: 1137-1144.
[20] Haneder S, Apprich SR, Schmitt B, Michaely HJ, Schoenberg SO, Friedrich KM and Trattnig S. Assessment of glycosaminoglycan content in intervertebral discs using chemical exchange saturation transfer at 3.0 Tesla: preliminary results in patients with low-back pain. Eur Radiol 2013; 23: 861-868.
[21] Kim M, Gillen J, Landman BA, Zhou J and van Zijl PC. Water saturation shift referencing (WASSR) for chemical exchange saturation transfer (CEST) experiments. Magn Reson Med 2009; 61: 1441-1450.
[22] Shrout PE and Fleiss JL. Intraclass correlations: uses in assessing rater reliability. Psychol Bull 1979; 86: 420-428.
[23] Cassinelli EH, Hall RA and Kang JD. Biochemistry of intervertebral disc degeneration and the potential for gene therapy applications. Spine J 2001; 1: 205-214.
[24] Wang SZ, Rui YF, Lu J and Wang C. Cell and molecular biology of intervertebral disc degeneration: current understanding and implications for potential therapeutic strategies. Cell Prolif 2014; 47: 381-390.
[25] Akella SV, Regatte RR, Gougoutas AJ, Borthakur A, Shapiro EM, Kneeland JB, Leigh JS and Reddy R. Proteoglycan-induced changes in T1rho-relaxation of articular cartilage at 4 T. Magn Reson Med 2001; 46: 419-423.
[26] Saar G, Zhang B, Ling W, Regatte RR, Navon G and Jerschow A. Assessment of glycosaminoglycan concentration changes in the intervertebral disc via chemical exchange saturation transfer. NMR Biomed 2012; 25: 255-261.
[27] Lotz JC, Haughton V, Boden SD, An HS, Kang JD, Masuda K, Freemont A, Berven S, Sengupta DK, Tanenbaum L, Maurer P, Ranganathan A, Alavi A and Marinelli NL. New treatments and imaging strategies in degenerative dis-

ease of the intervertebral disks. Radiology 2012; 264: 6-19.

[28] Bendtsen M, Bunger CE, Zou X, Foldager C and Jorgensen HS. Autologous stem cell therapy maintains vertebral blood flow and contrast diffusion through the endplate in experimental intervertebral disc degeneration. Spine (Phila Pa 1976) 2011; 36: E373-379.

[29] Allegri M, Montella S, Salici F, Valente A, Marchesini M, Compagnone C, Baciarello M, Manferdini ME and Fanelli G. Mechanisms of low back pain: a guide for diagnosis and therapy. F1000Res 2016; 5.